Research paper

Burning characteristics of aminoguanidinium 5,5′-azobis-1H-tetrazolate / ammonium nitrate as gas generating mixtures

Yasuyoshi Miyata[†], Masahiro Abe, Shingo Date, Makoto Kohga, and Kazuo Hasue

Department of Applied Chemistry, National Defense Academy, 1-10-20 Hashirimizu, Yokosuka, Kanagawa, 239-8686, JAPAN
[†]Corresponding address: g45077@nda.ac.jp

Abstract

Ammonium nitrate (AN) has been attracting attention as an oxidizer of gas generating mixtures. However, the gas generating mixtures that contain AN have the disadvantages that they are difficult to ignite, and that the burning rate is generally slow. In this study, aminoguanidinium 5,5'-azobis-1H-tetrazolate (AGAT), a tetrazole that could cause exothermic decomposition was used as a fuel, mixed with AN. To begin with, the initial decomposition of AGAT was examined by means of TG-DTA-MS. It was found that AGAT melted at 482 K, followed immediately by a dramatic decomposition, leading to 50 % weight loss. The decomposition of AGAT started from the cleavage of the heterocyclic ring which produced nitrogen and cyanamide with generation of heat. The burning rate of AGAT and AN mixture was also examined. Copper(II) oxide CuO or manganese dioxide MnO_2 that has been widely known as the decomposition catalyst of AN was added to the mixture to enhance the mass burning rate. The addition of CuO to the mixture enhanced the mass burning rate and decreased the pressure exponent of Vieille's equation, but the addition of MnO_2 did not enhance the mass burning rate. By means of thermocouples, the temperature profiles of the burning mixtures were also obtained and it was suggested that CuO may activate the reaction in the condensed phase reaction zone.

Keywords: Ammonium nitrate, Aminoguanidinium 5,5'-azobis-1H-tetrazolate, Copper (II) oxide, Temperature profile, Condensed phase.

1. Introduction

In this study, a new gas generating agent for airbags was studied. AN has been attracting attention over the years as an oxidizer for environment friendly, gas generating agents, because it does not generate the solid residues after burning and it is inexpensive. These merits could fulfill strict requirements imposed on gas generating agents for automobile airbag systems. However, AN has its disadvantages in that it is hygroscopic, which becomes a problem upon manufacturing and storage process, and that it goes through contraction and expansion during a series of phase transfer. There have been numerous studies [1]~[10] related to these problems, e.g. phase stabilization has been achieved by adding potassium nitrate and metal oxides to AN to make metal complexes and nitrate salts [11], [12]. Also, there is a problem that AN itself is difficult to burn, so that AN-based gas generating agents made by mixing with organic compound fuels have low burning rates. In the past, the authors have been studying on gas generating agents utilizing 5-amino-1H-tetrazaole (5-ATZ) [13]~[19]. However, because 5-ATZ undergoes endothermic decomposition, it does not readily burn by itself. Since AN also does not readily burn by itself, 5-ATZ is not favorable as a fuel when AN serves as an oxidizer. Accordingly, in this study, AGAT which is a tetrazole compound that can be self-decomposed by ignition has been used as a fuel to mix with AN. To the best of author's knowledge, the thermal decomposition of AGAT has not been researched yet. Therefore, we decided to investigate the thermal decomposition of AGAT. In addition, to enhance low burning rate of AN-based gas generating agent, we added CuO or MnO_2 that has been widely known as the decomposition catalyst of AN [20].

The purposes of this study are to clarify the thermal decomposition process of AGAT and to investigate the effects of decomposition catalyst on the burning of AGAT / AN.
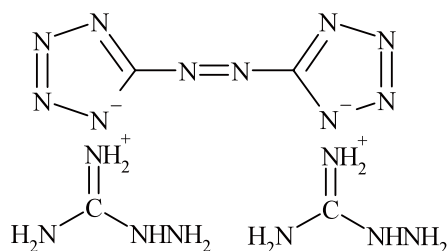
Fig. 1 Aminoguanidinium 5, 5'-azobis-1H-tetrazolate (AGAT).

Table 1 Compositions of gas generating agents.

Sample	AGAT	AN	CuO	MnO$_2$
A	50	50	—	—
B	50	50	5	—
C	50	50	—	5

Unit: (wt %)

2. Experimental

2.1 Samples

Figure 1 gives the structural formula of AGAT (Toyo Kasei Kogyo Co., Ltd). After drying AN (Kanto Chemical Co., Inc, JIS special grade reagent) at 333 K for 24 hours in a vacuum drier, it was milled with a vibration ball mill, and it was sieved through Japanese Industrial Standards (JIS) sieves. AGAT was also dried in a vacuum drying oven and sieved. AN of the particle size in the range of 150 – 300 μm and AGAT of the particle size in the range of 45 – 75 μm were used. The samples were mixed by the compositions as shown in Table 1.

2.2 Burning test

A cylindrical pellet (diameter: 10.15 mm) was prepared by compressing approximately 1.5 g mixture (particle size range of 45 - 75 μm) at 402 MPa for 5 minutes while embedding K-type (alumel-chromel) thermocouple (diameter: 50 μm). The sides of the pellet were coated with epoxy resin as a restrictor to achieve end-burning. The sample was ignited inside the chimney-type burner in which the internal pressure was controlled between 0.5 – 5 MPa. The details of the instrumentation are described elsewhere [13], [15]. The burning test was conducted to measure mass burning rates (m) and temperature profiles.

2.3 Thermal analysis

The melting point of AGAT was measured by a melting point apparatus BY-2 (Yazawa kagaku Co. Ltd.). The thermal decomposition processes were measured by thermogravimetry (TG) and differential thermal analysis (DTA) using Shimadzu DTG-50H. Simultaneously, mass spectrometry (MS) was conducted using Shimadzu QP-5000 to qualitatively analyze the gases produced by thermal decomposition. TG-DTA-MS analysis was conducted at the heating rate of 20 K min^{-1} in helium atmosphere (flow rate: 40 ml min^{-1}). In addition, the thermal decomposition processes were measured by differential scanning calorimetry (DSC)
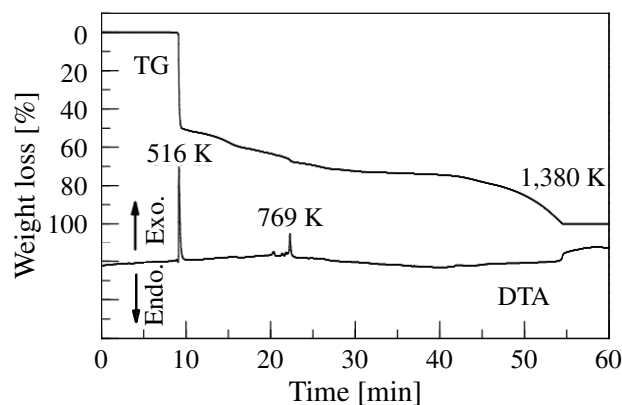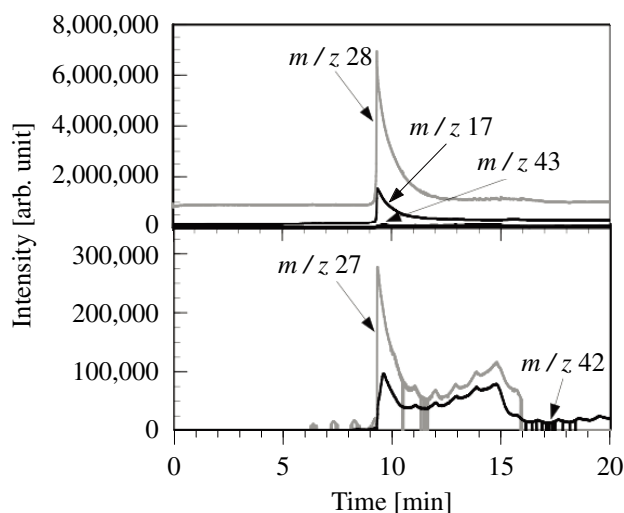

Fig. 2 TG-DTA curve of AGAT.
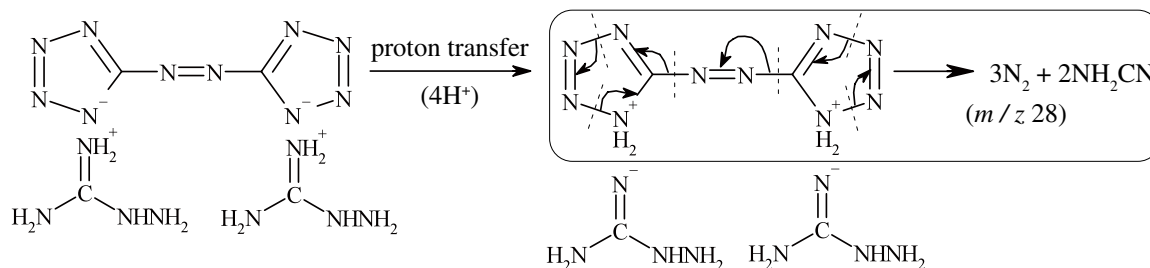

Fig. 3 MS data of decomposition products of AGAT.

using Shimadzu DSC-50. DSC analysis was conducted at the heating rate of 5 K min^{-1} in nitrogen atmosphere (flow rate 20 ml min^{-1}) using aluminum cell.

3 Results and Discussion

3.1 Thermal decomposition of AGAT

The first decomposition of AGAT was suggested to begin with the cleavage of the tetrazole rings with heat release, to produce nitrogen, ammonia and hydrogen cyanide. Figure 2 shows the TG-DTA curve of AGAT. From Figure 2, many steps of weight loss were observed in the TG curve and one sharp exothermic peak was observed in the DTA curve. The first decomposition occurred at 516 K, in which about 50 wt% of AGAT was decomposed. The whole decomposition completed at 1384 K.

Figure 3 shows the results of MS data at the first decomposition of AGAT. In general, derivatives of a tetrazole ring decompose by the cleavage of the ring [21], [22]. In addition, it is known that derivatives of a tetrazole ring decompose by two alternative mechanisms with a formation of nitrogen or azide [21], [23~25]. Formation of nitrogen (m / z 28) or azide (e.g. hydrogen azide HN$_3$ m / z 43) is caused by breakage of the single bond of a tetrazole ring. According to Fig. 3, a large amount of m / z 28 has been generated than m / z 43 at the first decomposition of AGAT. The signal of m / z 28 seems to have two candidates for the
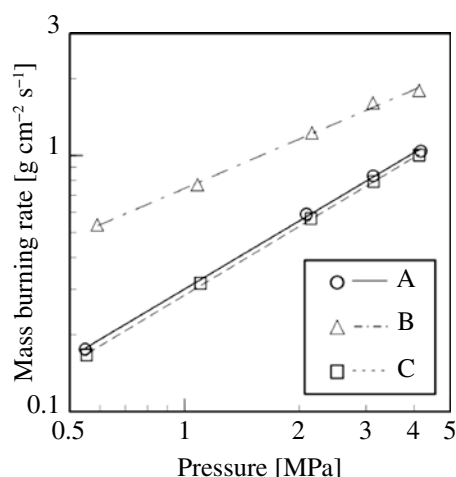
Scheme. 1   Decomposition pathway for AGAT.

Fig. 4   Mass burning rate for gas generating agents.

Table 2   Values of a_m and n of the Vieille's law.

Sample	a_m	n
A	0.301	0.884
B	0.745	0.640
C	0.285	0.893

parent species, namely nitrogen (N_2) and carbon monoxide (CO). However, because O is not included in the structural formula of AGAT, it is suggested that m/z 28 is N_2. This indicates that the first decomposition of AGAT involves a mechanism that forms N_2.

Scheme 1 shows the decomposition pathways for AGAT. The molecular structure of the first peak at m/z 42 is suggested to be cyanamide (NH_2CN) which suggests to have generated from the breakage of C − N bond in the aminoguanidinium anion (see Scheme 1). The two peaks at m/z 27 and m/z 42 appeared at the same time. This indicates that m / z 27 is a fragment of m/z 42. The molecular structure of m/z 27 is considered to be hydrogen cyanide (HCN). It is suggested that HCN is generated from the decomposition of NH_2CN (m/z 42) according to the following gas phase reaction.

$$2NH_2CN \rightarrow 2/3\ NH_3 + 2HCN + 2/3\ N_2$$

The theoretical weight fraction of N_2, NH_3, and HCN within the AGAT molecule (53.5 wt%) was found approximately equal to the observed weight loss (about 50 wt%). This is quite consistent with the opening of the azo tetrazolate ring. As a result, the first decomposition of AGAT seemed to begin with the cleavage of the tetrazole ring, to produce N_2, NH_3, and HCN.
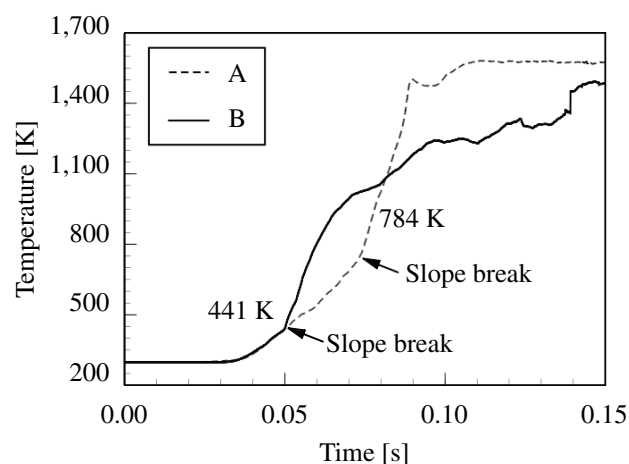

Fig. 5   Temperature profile at 4 MPa.

3.2 Effects of decomposition catalyst
3.2.1 Mass burning rate

Figure 4 shows the results of log-log plot of pressure versus m for gas generating agents. The addition of CuO increased m, but MnO_2 was not effective to increase m. m increased with pressure in the chimney-type burner and obey the Vieille's law. m could be expressed with the following equation

$$m = \rho r = \rho a P^n = a_m P^n \tag{1}$$

where ρ is density, r is linear burning rate, P is the ambient pressure, a and a_m are constants, and n is the pressure exponent of the burning rate. Table 2 gives the values of a and n determined from Fig. 4. The values of n correspond to the gradients of curve fitted lines in Fig. 4. The addition of CuO increased the values of a and decreased the values of n. This indicates that CuO increased m and reduced the influence of pressure. However, the addition of MnO_2 hardly changed the values of a and n. In other words, MnO_2 hardly influences m.

3.2.2 Temperature profile

Combustion wave consists of solid phase, condensed phase, and gas phase (Fig. 7). Figure 5 shows the comparison between temperature profiles at 4 MPa for mixtures with and without CuO. The horizontal axis shows time and temperature gradient shows the heating rate. In the condensed phase, heat release increased by the addition of CuO. In Fig. 5, slope breaks on the temperature profiles were observed. The temperature of slope break on the temperature profile of sample A was 784 K. This temperature
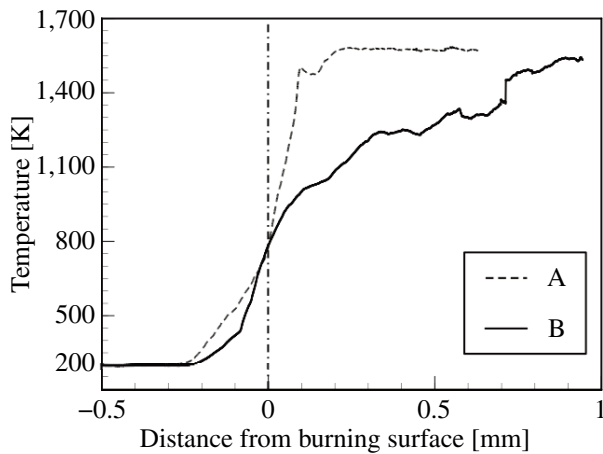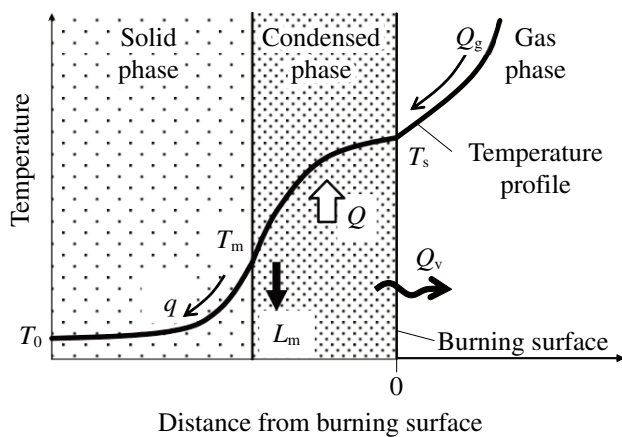
Fig. 6 Temperature profile at 4 M Pa.

Fig. 7 Schematic diagram of energy balance of combustion wave.

Fig. 8 DSC curves for mixtures.

is close to the dissociation temperature of AN which is 787 K at 4 MPa [26]. Accordingly, this temperature appears to be the burning surface temperature. The temperature of slope break on the temperature profile of sample B was 441 K. This temperature is close to the melting point of AN which is 442 K at 0.1 MPa [26]. The position of this temperature appears to be the boundary between solid phase and condensed phase. Up to this boundary temperature 441 K, the temperature profiles of sample A and sample B are almost the same. Such an agreement of temperature profile in the solid phase indicates that the burning rate control zone (BRCZ) may be located either in the condensed phase or in the gas phase. Above boundary temperature 441 K, a heating rate of sample B is larger than one of sample A. It is suggested that the addition of CuO increased the heat release in the condensed phase.

Figure 6 also shows the results of temperature profile at 4 MPa. The horizontal axis shows a distance from burning surface. The area on the right of the vertical dash-dotted line shows the gas phase. On the other hand, the area on the left shows the condensed phase and the solid phase. According to Fig. 6, the temperature gradient became small in the gas phase with an addition of CuO, and it suggested that the heat feedback from the flame decreased. On the other hand, the temperature gradient became steeper
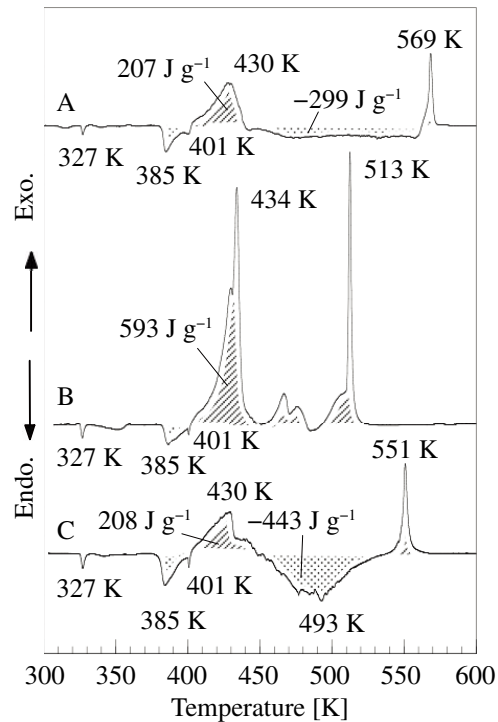
on the right hand of the burning surface. This transition indicates that the BRCZ may be either in the condensed phase or in the solid phase. Knowledge about the location of the BRCZ provides the means to obtain burning rate characteristics [27]. The experimental results of Fig. 5 and 6 indicate that the BRCZ may be in the condensed phase and that the addition of CuO decreases the thickness of the condensed phase and increase m.

Figure 7 shows the schematic diagram of energy balance of the combustion wave. T_s [K] is the burning surface temperature, T_0 [K] is the initial temperature (298 K), and T_m [K] is the boundary temperature between the solid phase and the condensed phase. Q_g [J g^{-1}] is the heat of feedback from the flame into the condensed phase by heat conductivity. Q [J g^{-1}] is the heat release in the condensed phase reaction layer. Q_v [J g^{-1}] is the heat of vaporization in the condensed phase. L_m [J g^{-1}] is the heat of fusion. The amount of heat transfer into the solid phase by the heat conduction, q [J g^{-1}] is calculated by the equation

$$q = Q_g + Q - L_m - Q_v \qquad (2)$$

In addition, from the temperature rise in the solid phase, q is also calculated by the equation

$$q = C\,(T_m - T_0) \qquad (3)$$

where C [J K^{-1} g^{-1}] is the specific heat in the condensed phase.
Hence, Q is calculated by the formula

$$Q = C\,(T_m - T_0) - Q_g + L_m + Q_v \qquad (4)$$

According to Fig. 6, the temperature gradient near the burning surface (ϕ) of sample A was 7.51×10^3 K m^{-1}, and ϕ of sample B was 2.74×10^3 K m^{-1}. Q_g [J g^{-1}] is calculated by the equation

$$Q_g = -\lambda \times \phi / m \qquad (5)$$

where λ is the thermal conductivity in the gas phase. According to eq. (5), Q_g of sample B is smaller than that of sample A. Additionally, C, T_m, T_0, L_m, and Q_v in eq. (4) are almost the same value for sample A and B. Therefore, Q of sample B is larger than that of sample A. The addition of CuO decreased Q_g and increased Q. As a result, m increased. The temperature profiles of AGAT / AN / CuO mixture indicate that the heat release in the condensed phase controls m.

3.2.3 Thermal analysis

In this chapter, the reactions in the condensed phase of the combustion wave were evaluated based on the DSC data. Figure 8 shows DSC curves for mixtures. According to the measurement by a melting point apparatus, the melting of AN occurred at 401 K which corresponds to the endothermic peak at 401 K of DSC curve. The addition of CuO promoted the exothermic decomposition in the range from about 400 K to 440 K. The addition of MnO_2 promoted the exothermic decomposition in the range from 493 K to 530 K on DSC curve of sample C in Fig. 8. However, MnO_2 increased the heat absorption in the condensed phase. This heat absorption suggests that MnO_2 absorb heat and does not react as a catalyst up to about 493 K. In addition, the temperatures of final peaks on DSC were 569 K (sample A), 513 K (sample B), and 551 K (sample C). These temperatures may indicate that CuO activates decomposition more prominently than MnO_2 in the condensed phase.

Based on DSC data, the addition of CuO activates the decomposition of AN and increases the heat release in the condensed phase. It is suggested that the increased heat feedback into the solid phase increases m.

4 Conclusions

The following conclusions were obtained through the investigations on the thermal decomposition of samples using TG-DTA-MS and DSC and on the combustion characteristics of samples through the measurement of temperature profile during burning test using chimney type burner and thermocouples.

(1) AGAT melted at 482 K, followed by an exothermal decomposition, corresponding to about 50 % weight loss.

(2) The first decomposition of AGAT appeared to begin with the cleavage of the tetrazole ring, to produce nitrogen and ammonia and hydrogen cyanide.

(3) The mass burning rate of AGAT / AN based mixtures follows Vieille's law.

(4) The addition of CuO promoted the decomposition of AN in the condensed phase and increased mass burning rate.

(5) The addition of CuO increased heat release in the condensed phase and decreased the thickness of the condensed phase.

(6) Mass burning rate of AGAT / AN / CuO mixtures have been controlled by the heat release in the condensed phase.

(7) The addition of MnO_2 did not increase the mass burning rate, may be because of an increase in heat absorption in the condensed phase.

References

 1) K. Hino, J. the Industrial Explosives Society (Sci. Tech. Energetic Materials), 8, 25 (1947).
 2) Y. Hosaka, J. the Industrial Explosives Society (Sci. Tech. Energetic Materials), 9, 2 (1948).
 3) S. Yamamoto and T. Sawada, J. the Industrial Explosives Society (Sci. Tech. Energetic Materials), 10, 160 (1949).
 4) S. Yamamoto and T. Sawada, J. the Industrial Explosives Society (Sci. Tech. Energetic Materials), 11, 240 (1950).
 5) J. Yoshida and H. Osada, J. the Industrial Explosives Society (Sci. Tech. Energetic Materials), 11, 101 (1950).
 6) I. Fukuyama, J. the Industrial Explosives Society (Sci. Tech. Energetic Materials), 16, 2 (1955).
 7) I. Fukuyama, J. the Industrial Explosives Society (Sci. Tech. Energetic Materials), 16, 218 (1955).
 8) I. Fukuyama, J. the Industrial Explosives Society (Sci. Tech. Energetic Materials), 17, 193 (1956).
 9) I. Fukuyama, J. the Industrial Explosives Society (Sci. Tech. Energetic Materials), 20, 119 (1959).
10) Y. Hara, T. Kodama and H. Osada, J. the Industrial Explosives Society (Sci. Tech. Energetic Materials), 33, 72 (1972).
11) C. Oommen and S. R. Jain, J. Propulsion and Power, 16, 133 (2000).
12) Jun-Hyung Kim, J. Chemical and Engineering, 30, 336 (1997).
13) K. Hasue, T. Akanuma, H. Houdai, and S. Date, Kayaku Gakkaishi (Sci. Tech. Energetic Materials), 60, 31 (1999).
14) K. Hasue, P. Boonyarat, Y. Miyata, and J. Takagi, Kayaku Gakkaishi (Sci. Tech. Energetic Materials), 62, 168 (2001).
15) Y. Miyata, S. Date, and K. Hasue, Propellants, Explosive, Pyrotechnics, 29, 247 (2004).
16) Y. Miyata, K. Baba, S. Date, and K. Hasue, Sci. Tech. Energetic Materials, 65, 167 (2004).
17) Y. Miyata, H. Kanou, S. Date, and K. Hasue, Sci. Tech. Energetic Materials, 66, 233 (2005).
18) Y. Miyata, S. Date and K. Hasue, Sci. Tech. Energetic Materials, 68, 125 (2007).
19) Y. Miyata, S. Date and K. Hasue, Sci. Tech. Energetic Materials, 68, 131 (2007).
20) H. Osada, "The Explosives Chemistry", p.359 (2003), MARUZEN.
21) J. Z. Wu, H. Yuzawa, T. Matsuzawa, M. Arai and M. Tamura, Kayaku Gakkaishi (Sci. Tech. Energetic Materials), 55, 66 (1994).
22) J. Z. Wu, J. M. Chen, M. Itou, M. Arai, M. Tamura, T. Andoh and S. Morisaki, Kayaku Gakkaishi (Sci. Tech. Energetic Materials), 55, 188 (1994).
23) A. I. Lesnikovich, S.V. Levchik, A. I. Balabanovich, O. A. Ivashkevich, G.V. Printsev and P. N. Gaponik, Thermochimica Acta, 200, 427 (1992).
24) S. Kawaguchi, M. Kumasaki, Y. Wada, M. Arai and M. Tamura, Kayaku Gakkaishi (Sci. Tech. Energetic Materials), 62, 16 (2001).
25) S.V. Levchik, A. I. Balabanovich, O. A. Ivashkevich, A. I. Lesnikovich, P. N. Gaponik and L. Costa, Thermochimica Acta, 225, 53 (1993).
26) V. P. Sinditskii, V. Y. Egorshev, D. Tomazi, and L. T. Deluca, The 7th International Symposium on Special Topics in Chemical Propulsion (7-ISICP), (2007), Paper, JAPAN.
27) L. K. Gusachenko and V. E. Zarko, Combustion, Explosion, and Shock Waves, 41, 20 (2005).

Aminoguanidinium 5,5'-azobis-1H-tetrazolate / 硝酸アンモニウムガス発生剤の燃焼特性

宮田泰好†，阿部雅浩，伊達新吾，甲賀　誠，蓮江和夫

　硝酸アンモニウムはガス発生剤の酸化剤として注目されてきた。しかし、硝酸アンモニウムを含むガス発生剤は、着火し難く、燃速が小さいという欠点がある。本研究では、発熱分解するテトラゾールであるaminoguanidinium 5,5'-azobis-1H-tetrazolate (AGAT)を燃料として使用し、硝酸アンモニウムと混合した。はじめに、AGATの第1分解をTG-DTA-MSで調べた。AGATは482 Kで融解した直後に、重量減少50 %に相等する分解をすることが分かった。AGATの分解は複素環の開裂で始まり、発熱を伴って窒素とシアナミドを生成した。AGATとANの混合物の燃焼速度も調べた。硝酸アンモニウムの分解触媒として知られている酸化銅(II)や酸化マンガン(IV)が質量燃速を増加させるために添加された。酸化銅(II)を添加すると質量燃速が増加し、Vieilleの式における圧力指数が減少したが、酸化マンガン(IV)を添加しても質量燃速は増加しなかった。熱電対により燃焼混合物の温度履歴も得られ、酸化銅(II)は凝縮相反応層において反応を促進すると考えられる。

防衛大学校応用化学群応用化学科　〒239-8686 神奈川県横須賀市走水1-10-20
†Corresponding address: g45077@nda.ac.jp